The Dependence of WAAS Ionospheric Error Bounds upon the Spatial Distribution of GPS Measurements

L. Sparks, A. Komjathy, and A.J. Mannucci

Jet Propulsion Laboratory, California Institute of Technology

BIOGRAPHY

Lawrence Sparks is a member of the Ionospheric and Atmospheric Remote Sensing Group (IARS) in the Tracking Systems and Applications Section at the NASA Jet Propulsion Laboratory (JPL). He received his Ph.D. in Applied Physics from Cornell University. His published research has spanned fields including fusion plasma physics, solar magnetohydrodynamics, atmospheric radiative transfer, and ionospheric modeling. He is currently working on applications of the Global Positioning System (GPS) to ionospheric science and is a member of the WAAS Integrity and Performance Panel (WIPP).

Attila Komjathy is currently a staff member of the IARS group specializing in remote sensing techniques using the Global Positioning System. Prior to his joining JPL in July 2001, he worked on the utilization of GPS reflected signals as a Research Associate at the University of Colorado's Center for Astrodynamics Research. He received his Ph.D. from the Department of Geodesy and Geomatics Engineering of the University of New Brunswick, Canada in 1997. He is a member of the WIPP.

Anthony J. Mannucci is the supervisor of the IARS group. He specializes in developing and applying ionospheric calibrations systems for deep space tracking and Earth science applications. He holds a Ph.D. in physics from UC Berkeley and is also a member of the WIPP.

ABSTRACT

To attain a higher level of service, the Wide Area Augmentation System (WAAS) for airline navigation must estimate ionospheric delays of Global Positioning System (GPS) signals more accurately and bound their errors more tightly. Undetected ionospheric irregularities that arise under disturbed conditions can become a major source of user delay error. To protect the user from such errors, the error bounds to be broadcast are augmented by an amount derived from an *ionospheric threat model*. This paper examines the dependence of the threat model upon the spatial distribution of GPS measurements.

Spatial configurations of GPS measurements can be characterized in terms of *spread metrics*. A spread metric gauges the degree to which a given set of measurements covers a given region densely and uniformly. A new metric is introduced here to distinguish more reliably measurement configurations that might fail to sample a significant ionospheric irregularity. Using the new metric to parameterize the spatial threat model, we show that the magnitude of the broadcast error bounds can be reduced. In our initial study the augmentation of the broadcast error bounds that protect the user from undersampled irregularities is reduced, on average, by 32%.

INTRODUCTION

The current implementation of the Wide Area Augmentation System (WAAS) for airline navigation is designed to meet the requirements for Lateral Navigation/Vertical Navigation (LNAV/VNAV) service (RTCA, 1996). A major obstacle to achieving a higher level of service is the need to estimate ionospheric delays of Global Positioning System (GPS) signals more accurately and to bound their errors more tightly. In WAAS the delay error and error bounds at a user location are inferred from vertical ionospheric delay estimates, modeled at regularly spaced intervals in latitude and longitude, *i.e.*, at *ionospheric grid points* (IGPs). The vertical delay estimate at each IGP is determined from a planar fit of neighboring slant delay measurements, projected to vertical using the *thin shell* model. This model is known to provide accurate delay estimates under

quiet conditions. Under disturbed conditions, however, ionospheric irregularities can arise that can become, if not detected, major sources of user delay error. System integrity requires that such errors be bounded accurately with a high degree of confidence.

The accuracy of a given planar fit depends strongly upon the spatial distribution of *ionospheric pierce points* (IPPs), *i.e.,* the points where the measurement raypaths cross the ionospheric shell. A highly skewed distribution of IPPs presents the possibility that a region near or to one side of an IGP may be undersampled and that a significant ionospheric disturbance affecting a user could go undetected. To protect the user from the danger posed by undersampled irregularities, WAAS augments the error bounds that are broadcast for each vertical delay estimate at an IGP. The amount of this augmentation is derived from an *ionospheric threat model*. The spatial threat model is derived by systematically excluding data from planar fits of vertical delay measurements within a neighborhood of each ionospheric grid point (IGP). The excluded data are then used to evaluate the maximum fit residual as a function of two metrics that quantify the spatial spread of the measurements: (1) the radius of a circle, centered at the IGP, large enough to encompass the IPPs used in the fit, and (2) the ratio of the IPP centroid radius to the fit radius, where the IPP centroid radius defines the distance from the IGP to the centroid of the fit IPPs. This latter ratio, the *relative centroid*, is meant to characterize the degree to which the IPPs are distributed *uniformly* across the fit region. Its use has proven critical to successful WAAS operation.

The primary purpose of defining a spread metric is to identify IPP configurations that might fail to sample a significant ionospheric irregularity. The extent to which a given metric is successful in achieving this goal has a direct impact on the magnitude of the ionospheric error bounds or *grid ionospheric vertical error* (GIVE). Since the user must be protected from the possible effects of a poor IPP sampling distribution, any metric that tends to confuse "better" and "worse" distributions will cause the "better" distributions to be treated too conservatively, *i.e.,* a higher error bound will be broadcast than is actually warranted.

In this paper, we consider a new spread metric that offers, in contrast to the relative centroid, a greater sensitivity to the nature of the IPP distribution. This spread metric is designed to meet the following requirements: (1) the metric should be sensitive to the angular distribution of the IPPs about the IGP; (2) the contribution of a single IPP to the metric defined at a given IGP should decrease with separation distance; (3) the metric should improve monotonically as the number of IPPs increases; and, (4) the parameterization of the metric should permit control of its sensitivity to the variation of a single IPP location. An additional advantage of the new spread metric is the ease with which it may be incorporated into WAAS. Its implementation affects only the parameterization of the spatial threat model, and thus its impact on the analysis of the probability of broadcasting hazardously misleading information (HMI) is minimal.

We report the results of an initial study that has generated a spatial threat model using the new metric. We find that the contribution to the GIVE that protects against the threat of an undersampled irregularity ($\sigma_{undersampled\text{-}decorr}$) is reduced, on average, by 32%. Hence, we conclude that the new spread metric can aid WAAS performance by helping to define error bounds that are safe but not overly conservative.

In the sections that follow, we first review how WAAS currently deals with the threat of undersampled ionospheric irregularities. After discussing the limitations of the relative centroid as a spread metric, we describe the new spread metric and its dependence on two fixed parameters. Finally we provide an example where the new metric has been incorporated into the spatial threat model, and we discuss the consequent reduction in broadcast error bounds.

HOW WAAS HANDLES UNDERSAMPLING OF THE IONOSPHERE

This section provides brief reviews of (1) the algorithm used to estimate vertical delay at ionospheric grid points, (2) the metrics WAAS currently uses to characterize IPP distributions, and (3) the threat model used to bound the error posed by undersampled ionospheric irregularities.

Estimation of vertical delay at IGPs

The current WAAS algorithm for estimating the local vertical delay at each IGP is based upon the thin shell model of the ionosphere (see, for example, Mannucci *et al.*, 1999, Birch *et al.,* 2002). By treating the ionosphere as if it were collapsed into a shell at a specified height h, a slant delay measurement S may be related to an estimate V of the vertical delay at the IPP by a simple geometric factor:

$$S = M(\alpha, h) \cdot V \qquad (1)$$

where

$$M(\alpha,h)=\left[1-\left(\frac{R_e\cos\alpha}{R_e+h}\right)^2\right]^{-1/2} \qquad (2)$$

is the thin-shell obliquity factor dependent upon h, the earth radius R_e, and the elevation angle α.

WAAS IGPs are spaced uniformly at 5° intervals in the conterminous United States (10° in Alaska). To estimate the vertical delay at an IGP, measurements with IPPs near the IGP are projected to vertical and fit to a plane. All measurements with IPPs that lie within a minimum fit radius R_{min} are included in the fit. If the number of such measurements is less than N_{pts}, the fit radius is extended until it defines a circle that surrounds N_{pts} points. If a circle with a maximum fit radius of R_{max} fails to encompass N_{pts} points, the fit is performed with fewer points, provided that at least N_{min} lie within R_{max}.

Characterizing the spatial distribution of IPPs

The estimate of the local vertical delay at the IGP can be highly inaccurate when the distribution of IPPs in the vicinity of the IGP is poor, *i.e.*, when this distribution contains large gaps or the bulk of the IPPs lie to one side of the IGP (as will often be the case when dealing with IGPs near the edge of the WAAS grid). Thus it proves useful to define metrics that characterize the spatial distribution of the IPPs included in the fit. A useful set of metrics should be highly sensitive to the density and the uniformity of the IPP coverage in the fit domain.

As noted previously, WAAS currently uses two metrics to characterize an IPP configuration: the fit radius, and the ratio of the IPP centroid radius to the fit radius. As the fit radius increases, the IPP density decreases, which permits larger irregularities to escape detection. The fit radius may thus be regarded as a rough indicator of the mean IPP density. The relative centroid serves to measure the degree of uniformity provided by the IPP sampling. When IPPs are spaced uniformly throughout the fit domain, this metric vanishes; on the other hand, it approaches unity when IPPs congregate near a single point at the edge of the fit domain.

Figure 1 shows a typical distribution of metric values for fits at WAAS IGPs over the course of one day. In the analysis N_{pts}, N_{min}, $R_{min,}$ and R_{max} have been set to representative values: 30 points, 10 points, 800 km, and 2100 km, respectively. (Note: optimal values for these parameters have yet to be determined.) The distribution is characterized by broad peaks except when the fit radius is near R_{min}. Note that all tabulated counts concerning fits

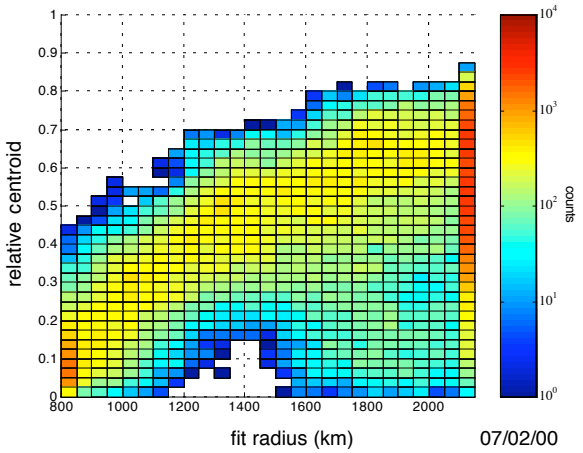

Figure 1. The distribution of relative centroid and fit radius for IPP configurations corresponding to slant TEC measurements recorded by WAAS receivers in the course of one day (July 2, 2000).

that include less than N_{pts} points (*i.e.*, the fit radius is R_{max}) are relegated to the final column.

The spatial threat model

To place an upper bound on the effects of undersampled irregularities, WAAS uses a spatial threat model that is designed to quantify a set of worst-case errors according to their dependence upon the IPP distribution. Since the threat due to undersampled irregularities is likely to be largest under disturbed conditions, such a threat model is developed using data recorded on days when significant ionospheric disturbances have occurred. The procedure for generating a threat model is summarized here (for more details, see Sparks *et al.*, 2001).

For a given epoch and a given IGP, a subset of the measurements is selected to represent possible user measurements, and these data are withheld from the fit. Subsequently the excluded measurements are projected to vertical and compared to the corresponding estimated values based upon the planar fit. Fit errors are tabulated only when *non-storm* (or *near-storm*) conditions exist, that is, only for fits that fail to trigger the storm detector. (The storm detector is based on a χ^2 "goodness-of-fit" statistic: local storm conditions are declared whenever the χ^2 of the planar fit exceeds a specified threshold; see Walter *et al.*, 2000).

This process is repeated for many other choices of subsets of excluded data. Two types of data deprivation domains are used: annular and three-quadrant. Fits that exclude data from annular regions about the IGP allow us

to assess the impact of localized spatial irregularities. A second deprivation domain excludes data from three quadrants of a rectangular (latitude-longitude) grid, whose origin lies on a diagonal passing through the IGP in question. Use of this type of domain serves to quantify errors that arise when the IPP distribution is skewed to one side of the IGP.

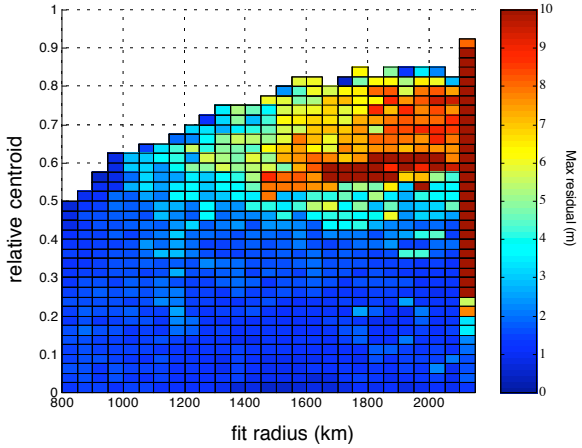

Figure 2. Maximum fit residual as a function of relative centroid and fit radius using the data deprivation algorithm applied to supertruth data from the following dates: January 11, 2000, April 6, 2000, April 7, 2000, July 15, 2000, July 16, 2000, and March 31, 2001.

Figure 2 displays pixel colors that represent the maximum error that occurs for a given fit radius and relative centroid. The data set used in the analysis consists of six days of slant delay measurements collected by the existing 25 WAAS Reference Stations on the following days: January 11, 2000, April 6, 2000, April 7, 2000, July 15, 2000, July 16, 2000, and March 31, 2001. On each of these days, the ionosphere experienced one or more strong disturbances. These data are first post-processed (1) to eliminate interfrequency biases, (2) to remove the effects of cycle slips in carrier phase measurements, (3) to level the carrier phase measurements to the corresponding range measurements, and (4) to filter spurious measurements by means of the redundancy provided by multiple receivers at each station. The resulting data, designated *supertruth*, contain minimal error due to measurement noise and range multipath.

Only points that lie within a 5° by 5° *threat domain* centered on the IGP are represented in Fig. 2. Again note that all tabulated errors concerning fits that include less than N_{pts} points are relegated to the final column. As expected, the behavior exhibited in the final column indicates that, as the number of points used in the fit drops below N_{pts}, the probability of large irregularities going undetected increases dramatically.

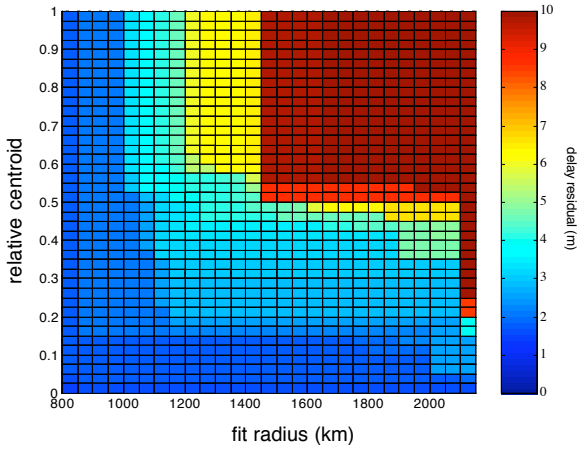

Figure 3. Overbound of maximum fit residuals displayed in Fig. 2, as a function of relative centroid and fit radius, used to calculate the augmentation to the error bounds due to the threat of undersampled irregularities.

Figure 3 presents an overbound of the previous figure, where the maximum delay error is required to be a monotonically increasing function of each metric and the resulting bounds have been increased by 10% to provide padding. From such an overbound WAAS determines the amount by which the broadcast error bounds must be augmented to protect against the possible presence of undetected irregularities. The mean value of this augmentation is determined by the frequency with which each region of the overbound is accessed, as specified by an IPP distribution such as that given in Fig. 1.

NEW SPREAD METRIC

Use of the relative centroid as an IPP spread metric has proven critical to permitting WAAS to meet performance specifications. Nevertheless, this metric possesses certain attributes that restrict its ability to distinguish IPP configurations that may fail to sample significant ionospheric irregularities. After enumerating these attributes, a new metric is proposed in this section that surmounts these limitations.

Limitations of relative centroid as a spread metric

A spread metric based upon the centroid of the IPP distribution will not be particularly sensitive to the angular distribution of IPPs about the IGP. For example, Fig. 4 shows six distinct IPP configurations that all have the same centroid (an IGP is assumed to coincide with the origin of each set of coordinate axes). Clearly the sampling of the region in the vicinity of the IGP is very different in each case, and the size of an irregularity that could go unsampled varies considerably from one case to another.

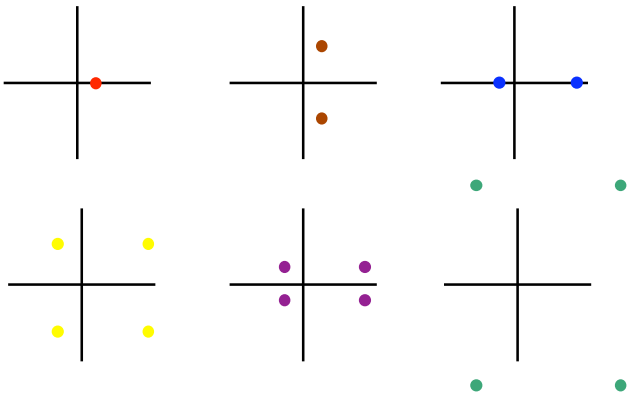

Figure 4. Six distinct IPP configurations that all have the same centroid.

Another limitation of a spread metric based upon the IPP centroid is that the contribution of a single IPP to the metric is complex and depends upon the number and placement of the other IPPs in the fit. In particular, adding a single IPP can make the coverage appear worse, *i.e.*, it can increase the magnitude of the centroid radius. Finally, there are no free parameters that allow one to adjust the sensitivity of the metric to the movement of a single IPP.

Definition of new spread metric

To overcome these limitations, we have defined a new metric to which each IPP in the fit contributes a distinct term. Let each IPP determine a pie-shaped wedge such that the line passing through the IPP and the IGP bisects the wedge (see Fig. 5). Specify that the width of the wedge diminish as the IPP moves away from the IGP. The metric then consists of the fraction of the area of the unit circle surrounding the IGP that is *not* covered by any of the pie-slices that constitute the fit. Good IPP coverage will then correspond to a metric value of zero, while poor coverage will have a metric value closer to unity. For

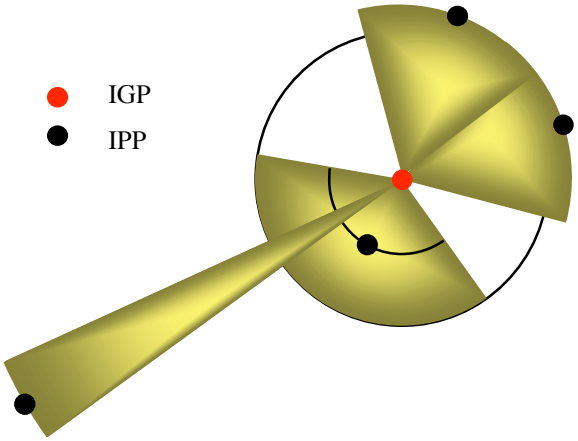

Figure 5. Schematic representation of the new spread metric. Each IPP defines a pie-shaped wedge that covers a portion of the unit circle. The metric is proportional to the area of the unit circle that remains uncovered.

example, the coverage represented in Fig. 5 corresponds to a metric value of approximately 0.3.

To make this definition more quantitative, define the angular spread of each pie-slice to be

$$s_i = \frac{2\pi}{A_{spd} + r_i^2 / R_{spd}^2}, \qquad (3)$$

where r_i is the distance from the IGP to the ith IPP (in km) and A_{spd} and R_{spd} are constants (A_{spd} is dimensionless; R_{spd} has units of km). We have chosen the asymptotic dependence of the metric to vary inversely with the square of the distance from the IGP. The spread metric at

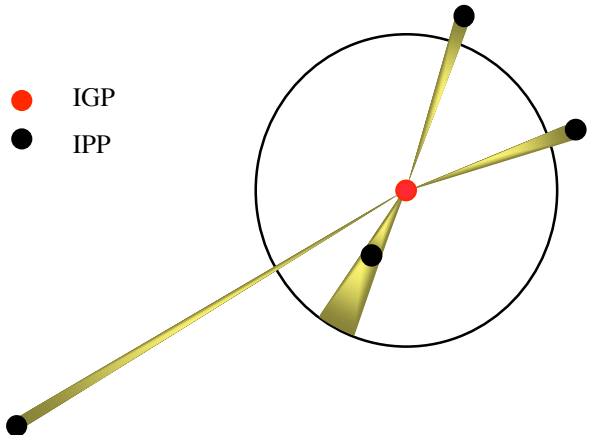

Figure 6. The same IPP configuration as in Fig. 5, using choices for A_{spd} and R_{spd} which give wedge widths that are too small.

a given IGP is then

$$M_{spd} = 1 - \frac{1}{2\pi} \sum s_i, \qquad (4)$$

where the summation is performed exclusive of overlap. Note that M_{spd} lies within the range

$$0 \le M_{spd} < 1. \qquad (5)$$

Proper choice of the constants A_{spd} and R_{spd} will be problem-dependent. The primary considerations that govern the choice of these constants are (1) the range of the number of points used in fits, and (2) the range of the fit radius. An inappropriate assignment of these constants can lead to wedge widths that are either too small (see Fig. 6), and, consequently, metric values will tend to congregate near unity, or too large (see Fig. 7), causing metric values to vanish. Ideally a proper choice of these constants will give rise to metric values that vary over a significant fraction of the interval between zero and one.

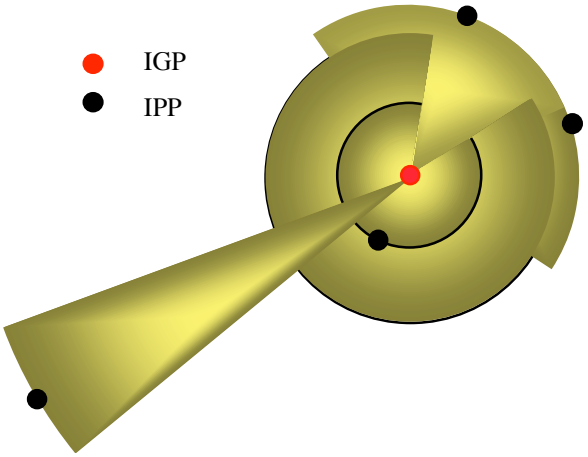

Figure 7. The same IPP configuration as in Fig. 5, using choices for A_{spd} and R_{spd} which give wedge widths that are too large.

A_{spd} controls the width of the wedge for an IPP that lies near the IGP. R_{spd} controls how rapidly the wedge width shrinks as the IPP moves away from the IGP. For two different choices of A_{spd} and three different choices of R_{spd} we have displayed in Fig. 8 the variation in the width of the pie slice as the IPP moves from the IGP to a distance of 2100 km from the IGP. Notice that making A_{spd} and R_{spd} larger tends to make the spread metric less sensitive to IPPs near the IGP.

By design this spread metric overcomes the limitations associated with the relative centroid. The metric is more sensitive to the angular distribution of the IPPs about the IGP than is the relative centroid. Furthermore, the contribution of a single IPP to the metric decreases with distance from the IGP, and the metric varies monotonically as the number of IPPs increases. Finally the parameterization of the metric permits control of its sensitivity to the variation of a single IPP location.

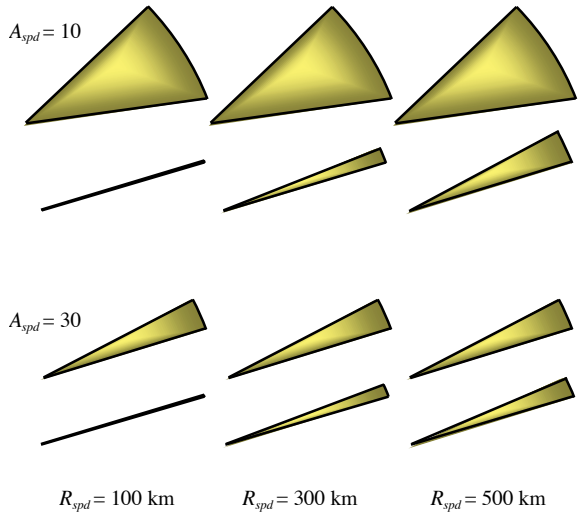

Figure 8. Ranges of IPP wedge widths for representative A_{spd} and R_{spd}. In each pair of wedges, the top wedge refers to an IPP near the IGP, and the lower wedge refers to an IPP at 2100 km.

We use a simple but quick algorithm for computing the new spread metric, an algorithm that provides an approximation of its analytic value. First, we define a grid of N_{spd} spokes emanating from the IGP and spaced uniformly. (In practice we set N_{spd} = 360.) For each IPP, a pie-shaped wedge is calculated, and any spoke lying within the wedge is eliminated from the set. After all IPPs have been processed, the metric is computed as 1 minus the fraction of spokes that remain in the set.

USING THE NEW SPREAD METRIC IN THE SPATIAL THREAT MODEL

The motivation for defining a new spread metric has been to identify more reliably IPP configurations that allow potentially significant ionospheric irregularities to go undetected. There are two distinct aspects to this problem. First, the choice of spread metric affects how IPP configurations are characterized (*e.g.,* see Fig. 1). Second, it affects how the fit residual overbound is characterized (*e.g.,* see Fig. 3). Changing the spread metric does not change the magnitudes of the fit residuals

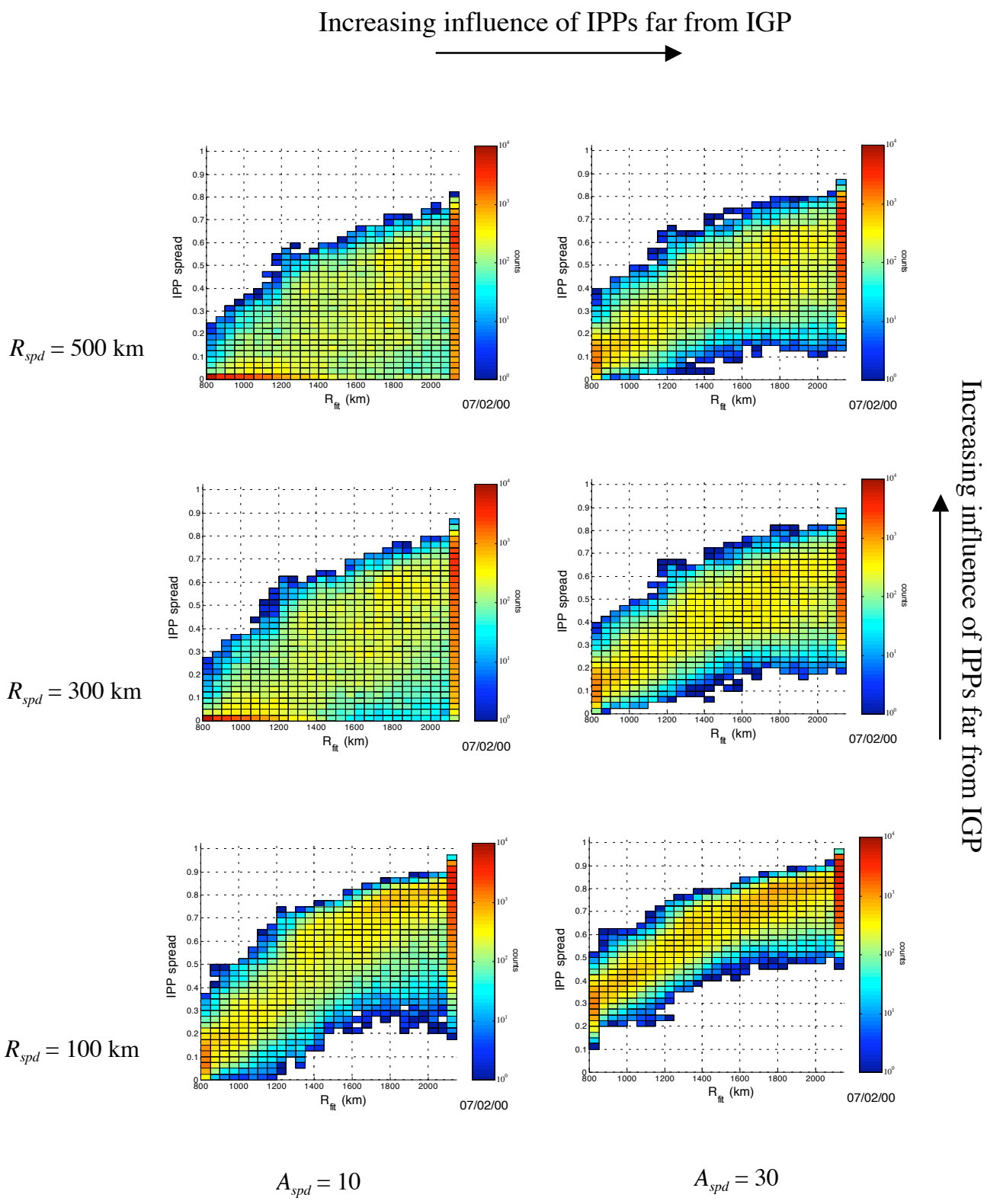

Figure 9. Distributions of IPP spread (M_{spd}) and fit radius for IPP configurations corresponding to slant TEC measurements recorded by WAAS receivers in the course of one day (July 2, 2000), using different values for the spread metric constants A_{spd} and R_{spd}. Arrows indicate changes in the metric constants that lead to an increasing influence of IPPs far from the IGP.

in which the counts are accrued. From the point of view of optimal WAAS performance, a *good* spread metric will tend to move the larger fit residuals to bins that are accessed less often. Such considerations will influence the optimal specification of constants in the new spread metric.

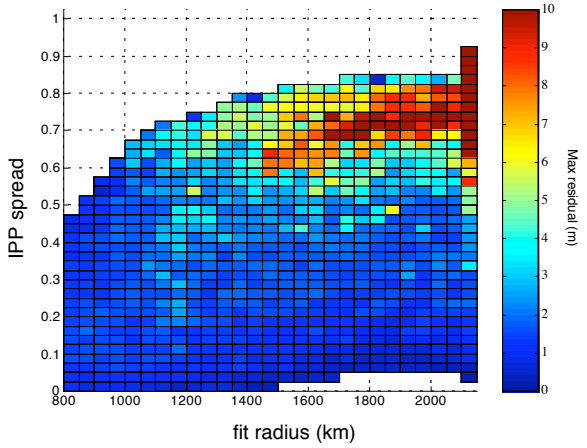

Figure 10. Maximum fit residual as a function of IPP spread (M_{spd}) and fit radius using the data deprivation algorithm applied to supertruth data from the following dates: January 11, 2000, April 6, 2000, April 7, 2000, July 15, 2000, July 16, 2000, and March 31, 2001.

For the same set of IPP configurations (*i.e.*, the same set of fits) used to generate Fig. 1, Fig. 9 shows distributions of metric values corresponding to different values for A_{spd} and and R_{spd}. Note that there is a stronger correlation between the value of the fit radius and the spread metric, especially when A_{spd} = 30, than there was

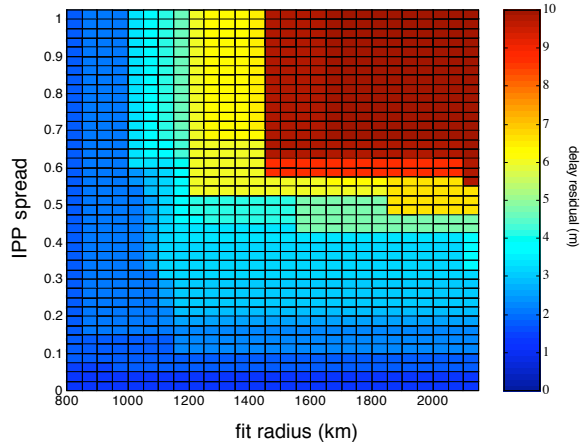

Figure 11. Overbound of maximum fit residuals displayed in Fig. 10, used to calculate $\sigma_{undersampled}$ as a function of IPP spread (M_{spd}) and fit radius.

when the relative centroid was used as the spread metric (Fig. 1). In other words, as the fit radius increases, the IPP coverage as measured by the new spread metric tends to get worse. In contrast, the relative centroid can remain good (*i.e.*, a metric value near zero) even as the fit radius increases, if the IPPs are spread around the IGP. Arrows are drawn in Fig. 9 to indicate that the influence of IPPs far from the IGP grows as A_{spd} and R_{spd} increase.

For several values of A_{spd} and R_{spd}, we have generated spatial threat models. To compare results, we evaluate the mean overbound that would be accessed by a given set of IPP configurations for a representative day (July 2, 2000). This mean value, $\overline{B}$, is calculated as follows:

$$\overline{B} = \frac{1}{N}\sum_{i,j} n_{ij} b_{ij}, \qquad (6)$$

where n_{ij} is the number of counts in the bin of the ith spread metric and jth fit radius (*e.g.*, see Fig. 1), b_{ij} is the corresponding overbound (*e.g.*, see Fig. 3), and N is the total number of counts in the distribution.

The lowest value of $\overline{B}$ achieved to date has been for A_{spd} set to 30 and R_{spd} set to 300 km. For these values the maximum fit residuals, tabulated as a function of spread metric and fit radius, are displayed in Fig. 10. The corresponding overbound is shown in Fig. 11. Comparing these figures to Figs. 2 and 3, we find that overbounds at a

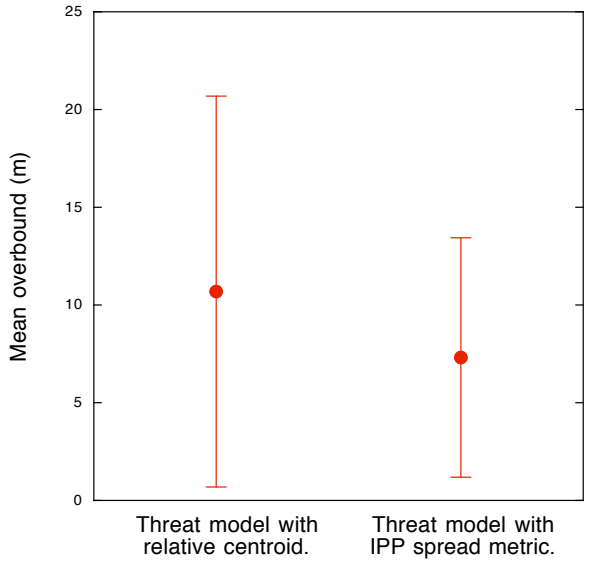

Figure 12. Mean overbounds accessed on July 2, 2000, using threat model based upon (a) relative centroid and (b) IPP spread metric. Also plotted are ranges specifying the standard deviations.

given level (*i.e.,* color) have tended to move to higher spread metric values. Comparing Fig. 1 and the distribution for A_{spd} = 30 and R_{spd} = 300 km in Fig. 9, we find distributions that are roughly comparable (except that the former contains some counts in the lower right-hand corner that are missing in the latter distribution, as discussed previously). Thus we should expect that, on average, the new distribution of spread metric values accesses regions of large overbounds less often, and this is indeed what we find. Figure 12 compares the mean overbound accessed and its standard deviation with the corresponding values for the threat model that uses the relative centroid as a spread metric. Using the new spread metric has reduced the mean overbound accessed by 32%. The contribution to the GIVE (designated $\sigma_{undersampled\text{-}decorr}$) that protects against the threat of an undersampled irregularity is proportional to the overbound. Thus, we should expect that it will also be reduced, on average, by a similar amount, depending upon precisely what data sets are used to generate the spatial threat model.

CONCLUSIONS

We have defined a new IPP spread metric designed to identify readily GPS measurement configurations that might fail to sample a significant ionospheric irregularity in the vicinity of a WAAS IGP. This metric exhibits the following attributes: (1) the metric is sensitive to the angular distribution of the IPPs about the IGP; (2) the contribution of a single IPP to the metric defined at a given IGP decreases with separation distance; (3) the metric improves monotonically as the number of IPPs increases; and, (4) the parameterization of the metric permits control of its sensitivity to the variation of a single IPP location.

Using this metric to parameterize the spatial threat model, we have shown that the magnitude of the error bounds broadcast by WAAS can be reduced. In particular the contribution to the GIVE that protects against the threat of an undersampled irregularity has been reduced, on average, by 32%. Thus, the new spread metric can aid WAAS performance by helping to define error bounds that are safe but not overly conservative.

An additional advantage of the new spread metric is the ease with which it may be implemented. Extensive analysis has already been performed on existing WAAS algorithms to ensure their reliability and safety. Whenever changes in operational algorithms are proposed, it is necessary to consider not only the difficulty of implementing the changes but also the impact on the analysis of the probability of broadcasting hazardously misleading information (HMI). The new spread metric affects only the parameterization of the spatial threat model, and thus its impact on the HMI analysis is minimal.

ACKNOWLEDGMENTS

The research described in this paper was performed by the Jet Propulsion Laboratory, California Institute of Technology, under contract with the National Aeronautics and Space Administration.

REFERENCES

Birch, M.J., J.K. Hargreaves, and G.J. Bailey, "On the use of an effective ionospheric height in electron content measurement by GPS reception", *Radio Sci.*, *37*(1), 1015, doi:10.1029/2000RS002601, 2002.

Mannucci, A.J., B.A. Iijima, U.J. Lindqwister, X. Pi, L. Sparks, B.D. Wilson, "GPS and Ionosphere" in *URSI Reviews of Radio Science, 1996-1999*, Oxford University Press, 1999.

RTCA Special Committee 159, *Minimum Operational Performance Standards for Global Positioning System/Wide Area Augmentation System Airborne Equipment, Doc. No. RTCA/DO-229*, RTCA, Inc., Washington, DC, January 1996.

Sparks, L., X. Pi, A.J. Mannucci, T. Walter, J. Blanch, A. Hansen, P. Enge, E. Altshuler, R. Fries, "The WAAS Ionospheric Threat Model," in *Proceedings of the International Beacon Satellite Symposium 2001*, Boston College, Boston, MA, June 3-6, 2001.

T. Walter, A. Hansen, J. Blanch, P. Enge, A.J. Mannucci, X. Pi, L. Sparks, B. Iijima, B. El-Arini, R. Lejeune, M. Hagen, E. Altschuler, R. Fries, A. Chu, "Robust Detection of Ionospheric Irregularities," in *Proceedings of the ION GPS 2000, 13th International Technical Meeting of the Institute of Navigation*, Salt Lake City, UT, September 11-14, 2000.